Polaritonic Enhancement of Near-field Scattering of Small Molecules Encapsulated in Boron Nitride Nanotubes: Chemical Reactions in Confined Space

Dániel Datz,[*,†,‡] Gergely Németh,[†,¶] Kate E. Walker,[§] Graham A. Rance,[‖] Áron Pekker,[†] Andrei N. Khlobystov,[§] and Katalin Kamarás[†]

†*Wigner Research Centre for Physics, Konkoly Thege Miklós út 29-33., Budapest, Hungary*
‡*Eötvös Loránd University, Pázmány Péter sétány 1/A, Budapest, Hungary.*
¶*Budapest University of Technology and Economics, Műegyetem rkp. 3., Budapest, Hungary.*
§*University of Nottingham, School of Chemistry, University Park, Nottingham, NG7 2RD, United Kingdom*
‖*Nanoscale & Microscale Research Centre, Cripps South, University of Nottingham, University Park, Nottingham NG7 2RD, United Kingdom*

E-mail: datz.daniel@wigner.hu

Abstract

Molecules encapsulated in nanotubes have been an interesting area of research for chemical reactions in confined spaces with huge potential for applications in the fields of hydrogen storage or targeted catalytic reactions.

We show that phonon polaritons of boron nitride nanotubes (BNNT) enhance the near-field vibrational spectra of molecules in close proximity to the surface. By encapsulating C_{60} fullerene in BNNTs, we can reach a sensitivity level of a few hundred molecules. Furthermore, we show by the photopolymerization of C_{60} that products of chemical reactions inside the tubes can be identified, so long as their vibrational signatures lie in the reststrahlen band of the BNNT.

Keywords

s-SNOM, encapsulation, BNNT, fullerene, near-field, enhancement, infrared, polariton

Chemical reactions in confined spaces have been explored with regard to various applications ranging from targeted catalytic reactions to quantum cascade lasers and high-energy technologies.[1] The outcome of these reactions is determined by multiple factors including the restricted number of orientations due to steric hindrance and also by the influence of the host system on the enclosed molecules. In this paper we demonstrate the possibility to investigate the products of chemical reactions between encapsulated molecules in nanosized cavities with 20 nm spatial resolution. This small-scale investigation allows us to study the correlation of chemical transformations with topology or other variables in the local environment.

The method of choice for the measurement is scattering type near-field optical microscopy (s-SNOM) which is a unique tool to analyze nanoscale optical phenomena in a variety of materials. The s-SNOM device (NeaSNOM, Neaspec GmbH) is an atomic force microscope using a metallic tip (Arrow-NCPt, Nanoworld)

in intermittent contact mode. Laser illumination is coupled in and focused on the tip by an off-axis parabolic mirror. Near-field information is isolated using an interferometric pseudo-heterodyne detection technique.[2] This detection scheme makes it possible to collect both the amplitude (A) and the phase (ϕ) of the scattered light resulting from the tip-sample interaction. The near-field absorption is calculated as $A_3 sin(\phi_3)$,[3,4] where the subscript refers to the demodulation on third harmonic of the vibrating AFM tip (see Supporting Information). Both amplitude and phase response of the scattered light from the sample are measured relative to the substrate. While any excitation that influences the scattered light could be detected by this method, most studies concentrate on collective excitations and their interferences. Advances were made on plasmon-polariton modes in graphene,[5,6] phonon-polariton modes in hexagonal boron nitride (hBN),[7–11] alpha-phase molybdenum trioxide (α-MoO_3)[12] and even the hybrid phonon-plasmon modes of stacked hBN-graphene systems.[13] In a previous publication[14] we identified clusters of a few hundred metal atoms in single-walled carbon nanotubes (SWNT) based on their free-electron (Drude) absorption. Molecular vibrations remained more elusive, most reports being about polymer films, macromolecules or molecules attached to an antenna surface.[15–19] Hyperspectral Raman measurements by Gaufrés et al.[20] set a lower detection limit of ten α-sexithiophene molecules encapsulated in SWNTs, but direct infrared detection at this scale has not yet been performed.

Here we present measurements on few-molecule scattering spectroscopy, specifically on C_{60} fullerene molecules encapsulated in boron nitride nanotubes (scheme in Fig. 1, for TEM images of the nanotubes after encapsulation see Supporting Information). Considerable enhancement of the near-field interaction is detected when the molecules are spatially confined in BNNTs. The enhancement makes it possible to follow chemical reactions in the confined space, by identifying the products of photopolymerization (dimers and trimers) based on their spectral bands in the reststrahlen band of the nanotubes.

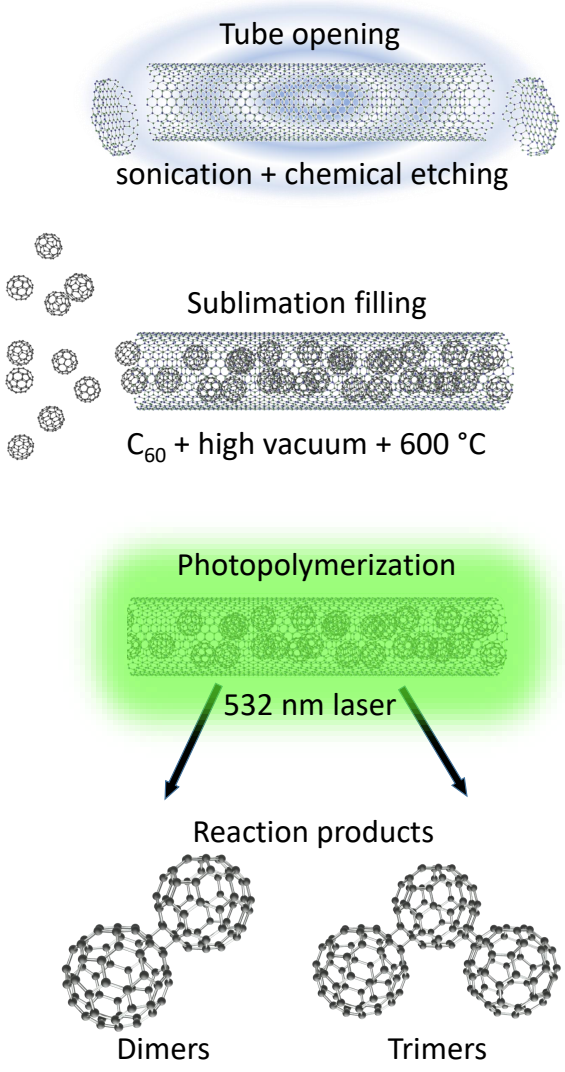

Figure 1: Schematic diagram showing the chemical steps presented in this article. The steps are as follows: cleaning and opening, encapsulation of C_{60} molecules and photopolymerization with 532 nm laser, resulting in presumably mostly dimerized and trimerized fullerene molecules

Layered materials such as hexagonal boron nitride show anisotropy in their dielectric function, thus the dielectric function is different for the in-plane and out-of-plane direction. Hexagonal boron nitride has two vibrational phonon modes in the mid-infrared region. Since BN is a polar material, the transverse and longitudinal vibrations are far apart in frequency, resulting in two reststrahlen bands (similar to

the reststrahlen band in bulk materials) characterized by $\Re(\epsilon_a) < 0$, where a refers to either the in-plane ($\|$) or the out-of-plane ($\perp$) component of the dielectric tensor. The anisotropy in hBN results in a scenario where in a given reststrahlen band only one of these two values is negative, while the other one is positive. The isofrequency curves in such a material are thus hyperbolic as opposed to ellipsoidic. In the reststrahlen band ranging from 1378 cm^{-1} to 1610 cm^{-1}, $\Re(\epsilon_\|) < 0$ and $\Re(\epsilon_\perp) > 0$ which describes an open hyperboloid and is referred to as Type-II hyperbolic response. In this region the dielectric function can be described by

$$\epsilon_a(\omega) = \epsilon_{a,\infty}\left(1 + \frac{\omega_{a,LO}^2 - \omega_{a,TO}^2}{\omega_{a,TO}^2 - \omega^2 - i\omega\gamma_a}\right) \quad (1)$$

where $a = \|, \perp$ and the parameters are $\epsilon_\infty = 4.52$, $\omega_{LO} = 1610\ cm^{-1}$, $\omega_{TO} = 1378\ cm^{-1}$ and $\gamma = 5\ cm^{-1}$.[19] To describe the optical properties of BNNTs, we treat the nanotubes as rolled-up hBN planes of one or two layers (see Supporting Information for TEM images), therefore in cylindrical coordinates $\epsilon_r = \epsilon_\perp$ and $\epsilon_\theta = \epsilon_z = \epsilon_\|$.[10] Phillips *et al.*[21] studied the dielectric function of BNNTs and treated the system as a hollow cylinder filled with air using an effective medium theory. In our case, since the diameter of our tubes is much smaller, effective medium approximation gives negligible correction.

In this upper reststrahlen band region, where hyperbolic phonon polaritons can propagate,[10] the electric field of the excited polariton is perpendicular to the nanotube surface. This orientation of the additional electric field aligns with the near field of the illuminated tip. We suggest that this interplay between the exciting and the polaritonic electric field causes the enhancement of the scattered signal originating not only from the nanotubes but also from the molecules inside.

Furthermore, the hyperbolic nature of the boron nitride nanotubes means that there is no cutoff frequency of the hyperbolic phonon polaritons that are allowed to propagate in the material. Since the hyperbolic phonon polariton wavelength is inversely proportional to the number of layers of the boron nitride host, in few-layered BNNTs this leads to extreme confinement of electromagnetic fields. These confined fields may explain the detected tip-induced hyperbolic phonon polariton resonant near-field coupling to the molecular vibrations.

Fig. 2 shows near-field absorption maps of a single, 3.5 nm diameter filled nanotube at three different illumination wavenumbers. At 1350 cm^{-1} no considerable contrast is seen as this wavenumber is below ω_{TO} and thus below the upper reststrahlen band. At the TO phonon wavenumber 1378 cm^{-1}, the near-field absorption contrast is rather high everywhere along the nanotube, as one would expect. At 1428 cm^{-1}, which corresponds to one of the T_{1u} absorption bands of C_{60}, high-contrast regions are observed along the nanotube, although less uniform than at the phonon mode frequency (1378 cm^{-1}). Since this signal is not present in non-filled nanotubes, we assign it to the encapsulated C_{60} molecular clusters. The results indicate efficient, albeit non-uniform filling.

To demonstrate the near-field enhancement effect of the BNNT, we have also measured C_{60} without the BNNT host. Fig. 3 shows the comparison of the near-field absorption signal of 8–10 nm high C_{60} islands with the filled and unfilled areas of the nanotube of Fig. 2. Spectra are acquired by tuning the infrared laser in the range 1330 – 1450 cm^{-1}. The optical signal values from measurement points taken above the silicon substrate are averaged and treated as the reference signal. Measurement points above the nanotube are also averaged and then normalized to the reference signal. Marked spots in Fig. 2b indicate the positions used for extraction of the spectra shown in Fig. 3. The fullerene absorption at 1428 cm^{-1} is missing from the measurements on the C_{60} islands despite the considerably higher amount of material under the tip. This confirms the amplification of the near-field signal measured in the presence of BNNT in the appropriate wavenumber range (above ω_{TO}).

To estimate the detection sensitivity obtained by encapsulation, we calculate the volume of the measured region and the number of C_{60} molecules actively participating in the near-

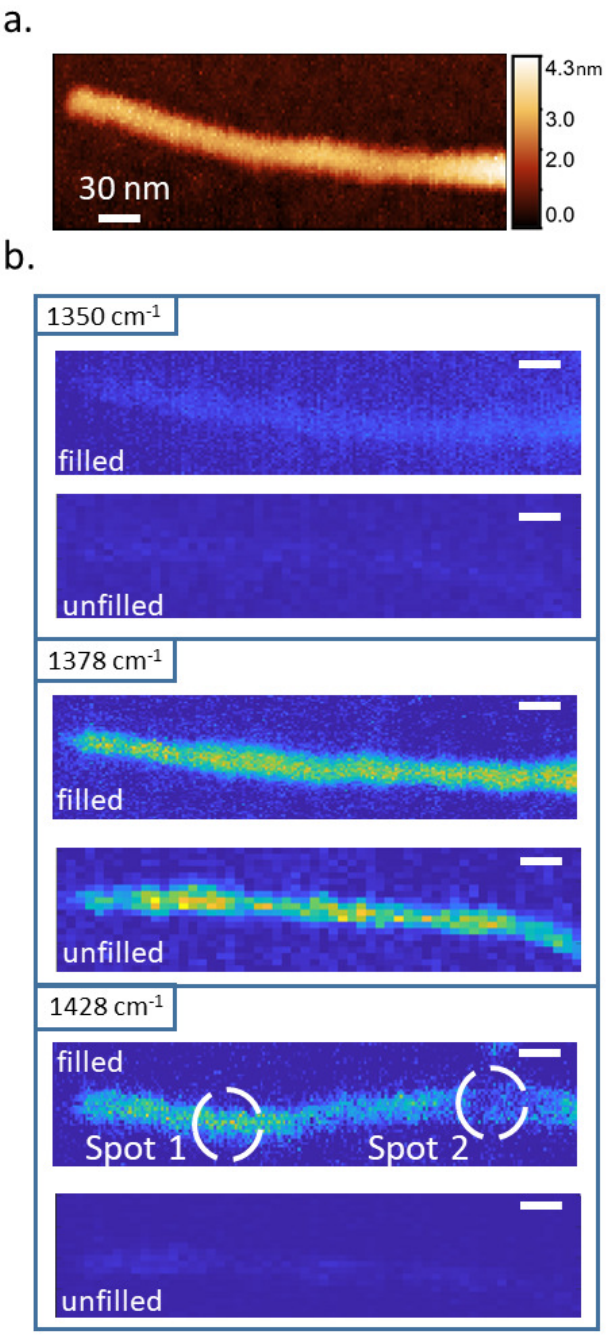

Figure 2: a. AFM image of the C_{60} filled nanotube. The nanotube diameter is approximately 3.5 nm. b. Optical absorption maps at three different wavenumbers. Absorption is calculated as described in the Supporting Information. At each wavenumber, the upper map is that of a filled nanotube while the lower map is of an unfilled one. On the 1428 cm^{-1} map marked spots indicate the positions where spectra were obtained (Fig. 3). The colorscale on all the optical maps is the same as on the respective (filled or unfilled) 1378cm^{-1} map.

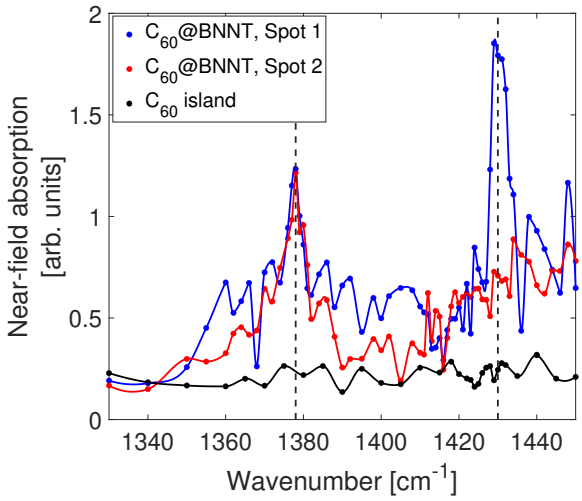

Figure 3: Near-field spectra measured on C_{60}@BNNT and C_{60} islands on Si. Spectra were measured at nanotube positions marked by the dashed circles in Fig. 2b. BNNT phonon modes (1378 cm^{-1}) and C_{60} modes (1428 cm^{-1}) are marked with vertical lines. Comparison with the spectrum measured on C_{60} islands shows the lack of both modes in the absence of BNNT.

field scattering process. An upper limit on the number of C_{60} molecules in the measured volume of the nanotube is approximately 160 (see Supporting Information).

As a reference, the black curve on Fig. **??** shows near-field measurements taken on C_{60} nanoislands of 10 nm height dropcasted on Si surface. Since without BNNT, no signal is detected at 1429 cm^{-1} no enhancement factor can be calculated.

To put this number in perspective, the same amount of C_{60} in a far-field measurement would give an absorption value in the 10^{-17} range,[22] clearly below the detection limit of any far-field spectroscopic method.

In an attempt to identify further encapsulated species, we have induced a photopolymerization reaction between the C_{60} molecules using a visible (532 nm) laser focused on the near-field measurement spot. After the initial measurement of the original C_{60}@BNNT system we illuminated the same spot with the visible laser for 5 hours, then carried out an identical near-field spectroscopy scan. Upon illumination with the laser, C_{60} molecules undergo photopolymeriza-

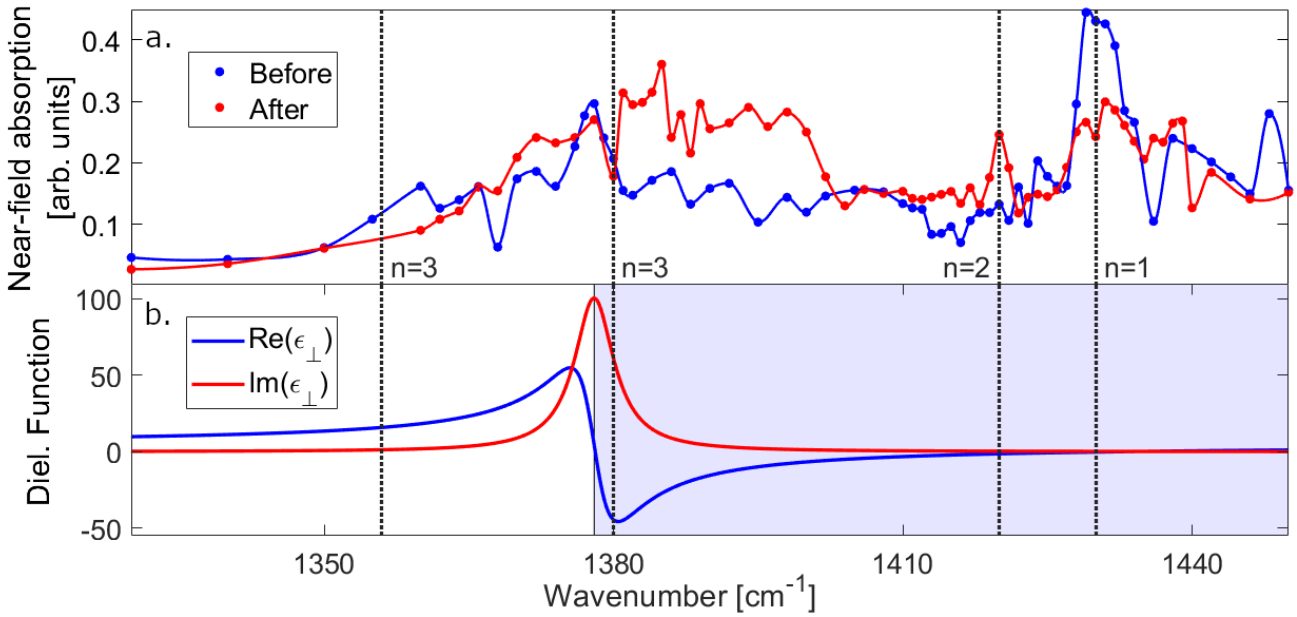

Figure 4: a) Spectra taken on the same section of a C_{60}@BNNT before and after intense green laser illumination. Vertical lines show the vibrational modes of different oligomers of C_{60}, where n denotes the degree of polymerization. New, narrow peaks appear at wavenumbers corresponding to polymerized C_{60} denoted by the vertical lines at 1360, 1385 (n=3), 1420 (n=2) and 1429 (n=1) wavenumbers. The $(C_{60})_3$ trimer mode outside of the reststrahlen band does not give a new peak. b) Boron nitride dielectric function, showing the lower energy side of the upper reststrahlen band (shaded region). The modes in the shaded reststrahlen band region are detectable, while the trimer mode outside is not.

tion resulting mainly in photodimers and phototrimers. The photopolymerization products have distinctive vibrational features that were studied extensively by far-field techniques.[23–28] Fig. 4a compares results before and after illumination. The C_{60} monomer peak is still visible but an additional mode appears at 1420 cm^{-1} and the peak around 1378 cm^{-1} becomes split and heavily distorted. According to DFT calculations and measurements from reference 29, these peaks correspond to dimer and trimer absorption modes. The complexity of the higher trimer peak and the nanotube peak may be caused by interaction between the two vibrational modes. It is important to note that the lower trimer absorption band does not appear in our spectrum, as the energy of this vibration is outside of the reststrahlen band, as seen in Fig. 4b.

The absence of vibrational features below ω_{TO} confirms the active role of BNNT in the near-field absorption process, by providing the robust phonon-polariton excitation close to the molecular excitations. The interacting, coupled excitations (approximated by harmonic oscillators) may result in the observed enhancement. The electronic field at the surface of the nanotubes in the reststrahlen band region is perpendicular to the surface, resulting in better coupling to the molecular excitations.

In conclusion, we have shown that small-molecule infrared spectroscopy on only hundreds of molecules is possible if the absorption process is supported by the phonon-polariton mode of the encapsulating boron nitride nanotube. The boron nitride cavity also enables observation of few-molecule chemical processes (in this case photopolymerization), that is especially interesting for improving the insight into more industrial areas such as hydrogen storage, spintronics and energy-related applications.[1] The simplicity of the filling process makes filled boron nitride nanotubes appealing candidates for the investigation of chemical pro-

cesses in nanotubes.

Acknowledgement We thank Béla Pécz for the TEM images. We would like to thank the Nanoscale & Microscale Research Centre (nmRC), University of Nottingham, for enabling access to HRTEM instrumentation. This research was funded by the Hungarian National Research Fund (OTKA) through grant nos. SNN 118012, PD 121320 and FK 125063. Research infrastructure was provided by the Hungarian Academy of Sciences (MTA).

Supporting Information Available

Description of experimental details, s-SNOM setup, HRTEM images, estimation of number of molecules measured, additional measurement of near-field absorption

References

(1) Manzetti, S. Molecular and crystal assembly inside the carbon nanotube: encapsulation and manufacturing approaches. *Adv. Manuf.* **2013**, *1*, 198–210.

(2) Ocelic, N.; Huber, A.; Hillenbrand, R. Pseudoheterodyne detection for background-free near-field spectroscopy. *Appl. Phys. Lett.* **2006**, *89*, 101124.

(3) Xu, X. G.; Tanur, A. E.; Walker, G. C. Phase Controlled Homodyne Infrared Near-Field Microscopy and Spectroscopy Reveal Inhomogeneity within and among Individual Boron Nitride Nanotubes. *J. Phys. Chem. A* **2013**, *117*, 3348—-3354.

(4) Xu, X. G.; Ghamsari, B. G.; Jiang, J.-H.; Gilburd, L.; Andreev, G. O.; Zhi, C.; Bando, Y.; Golberg, D.; Berini, P.; Walker, G. C. One-dimensional surface phonon polaritons in boron nitride nanotubes. *Nat. Commun.* **2014**, *5*, 4782–1–6.

(5) Fei, Z.; Rodin, A. S.; Andreev, G. O.; Bao, W.; McLeod, A. S.; Wagner, M.; Zhang, L. M.; Zhao, Z.; Thiemens, M.; Dominguez, G.; Fogler, M. M.; Castro Neto, A. H.; Lau, C. N.; Keilmann, F.; Basov, D. N. Gate-tuning of graphene plasmons revealed by infrared nano-imaging. *Nature* **2012**, *487*, 82–85.

(6) Gerber, J. A.; Berweger, S.; O'Callahan, B. T.; Raschke, M. B. Phase-resolved surface plasmon interferometry of graphene. *Phys. Rev. Lett.* **2014**, *113*, 055502.

(7) Dai, S. et al. Tunable phonon polaritons in atomically thin van der Waals crystals of boron nitride. *Science* **2014**, *343*, 1125–1129.

(8) Li, P.; Lewin, M.; Kretinin, A. V.; Caldwell, J. D.; Novoselov, K. S.; Taniguchi, T.; Watanabe, K.; Gaussmann, F.; Taubner, T. Hyperbolic phonon-polaritons in boron nitride for near-field optical imaging and focusing. *Nat. Commun.* **2015**, *6*, 1–9.

(9) Li, P.; Dolado, I.; Alfaro-Mozaz, F. J.; Nikitin, A. Y.; Casanova, F.; Hueso, L. E.; Vélez, S.; Hillenbrand, R. Optical nanoimaging of hyperbolic surface polaritons at the edges of van der Waals materials. *Nano Lett.* **2017**, *17*, 228–235.

(10) Zhou, Y.; Qi, D.-X.; Wang, Y.-K. Phonon polaritons in cylindrically curved h-BN. *Opt. Express* **2017**, *25*, 17606–17615.

(11) Dai, S. et al. Phonon polaritons in monolayers of hexagonal boron nitride. *Adv. Mater.* **2019**, *31*, 1806603.

(12) Zheng, Z.; Chen, J.; Wang, Y.; Wang, X.; Chen, X.; Liu, P.; Xu, J.; Xie, W.; Chen, H.; Deng, S.; Xu, N. Highly confined and tunable hyperbolic phonon polaritons in van der Waals semiconducting transition metal oxides. *Adv. Mater.* **2018**, *30*, 1705318.

(13) Woessner, A.; Lundeberg, M. B.; Gao, Y.; Principi, A.; Alonso-González, P.; Carrega, M.; Watanabe, K.; Taniguchi, T.; Vignale, G.; Polini, M.; Hone, J.; Hillenbrand, R.; Koppens, F. H. L. Highly confined low-loss plasmons in graphene–boron nitride heterostructures. *Nat. Mater.* **2015**, *14*, 421–425.

(14) Németh, G.; Datz, D.; Pekker, Á.; Saito, T.; Domanov, O.; Shiozawa, H.; Lenk, S.; Pécz, B.; Koppa, P.; Kamarás, K. Near-field infrared microscopy of nanometer-sized nickel clusters inside single-walled carbon nanotubes. *RSC Adv.* **2019**, *9*, 34120–341244.

(15) Aizpurua, J.; Taubner, T.; de Abajo, F. J. G.; Brehm, M.; Hillenbrand, R. Substrate-enhanced infrared near-field spectroscopy. *Opt. Express* **2008**, *16*, 1529–1545.

(16) Neubrech, F.; Pucci, A.; Cornelius, T. W.; Karim, S.; García-Etxarri, A.; Aizpurua, J. Resonant plasmonic and vibrational coupling in a tailored nanoantenna for infrared detection. *Phys. Rev. Lett.* **2008**, *101*, 157403–1–4.

(17) Neubrech, F.; Weber, D.; Enders, D.; Nagao, T.; Pucci, A. Antenna sensing of surface phonon polaritons. *J. Phys. Chem. C* **2010**, *114*, 7299–7301.

(18) Neubrech, F.; Huck, C.; Weber, K.; Pucci, A.; Giessen, H. Surface-enhanced infrared spectroscopy using resonant nanoantennas. *Chem. Rev.* **2017**, *117*, 5110–5145.

(19) Autore, M.; Li, P.; Dolado, I.; Alfaro-Mozaz, F. J.; Esteban, R.; Atxabal, A.; Casanova, F.; Hueso, L. E.; Alonso-González, P.; Aizpurua, J.; Nikitin, A. Y.; Vélez, S.; Hillenbrand, R. Boron nitride nanoresonators for phonon-enhanced molecular vibrational spectroscopy at the strong coupling limit. *Light Sci. Appl.* **2018**, *7*, 17172–1–8.

(20) Gaufrès, E.; Tang, N. Y.-W.; Favron, A.; Allard, C.; Lapointe, F.; Jourdain, V.; Tahir, S.; Brosseau, C.-N.; Leonelli, R.; Martel, R. Aggregation control of α-sexithiophene via isothermal encapsulation inside single-walled carbon nanotubes. *ACS Nano* **2016**, *10*, 10220–10226.

(21) Phillips, C.; Gilburd, L.; Xu, X. G.; Walker, G. C. Surface and volume phonon polaritons in boron nitride nanotubes. *J. Phys. Chem. Lett.* **2019**, *10*, 4851–4856.

(22) Iglesias-Groth, S.; Cataldo, F.; Manchado, A. Infrared spectroscopy and integrated molar absorptivity of C_{60} and C_{70} fullerenes at extreme temperatures. *Mon. Not. R. Astron. Soc.* **2011**, *413*, 213–222.

(23) Rao, A. M.; Zhou, P.; Wang, K.-A.; Hager, G. T.; Holden, J. M.; Wang, Y.; Lee, W.-T.; Bi, X.-X.; Eklund, P. C.; Cornett, D. S.; Duncan, M. A.; Amster, I. J. Photoinduced polymerization of solid C_{60} films. *Science* **1993**, *259*, 955–957.

(24) Rao, A. M.; Eklund, P. C.; Hodeau, J.-L.; Marques, L.; Nunez-Regueiro, M. Infrared and Raman studies of pressure-polymerized C_{60}. *Phys. Rev. B* **1997**, *55*, 4766.

(25) Iwasa, Y.; Tanoue, K.; Mitani, T.; Yagi, T. Energetics of polymerized fullerites. *Phys. Rev. B* **1998**, *58*, 16374–16377.

(26) Pusztai, T.; Oszlányi, G.; Faigel, G.; Kamarás, K.; Gránásy, L.; Pekker, S. Bulk structure of phototransformed C_{60}. *Solid State Commun.* **1999**, *111*, 595–599.

(27) Kováts, É..; Oszlányi, G.; Pekker, S. Structure of the crystalline C_{60} photopolymer and the isolation of its cycloadduct components. *J. Phys. Chem. B* **2005**, *109*, 11913–11917.

(28) Klupp, G.; Borondics, F.; Kováts, É..; Pekker, Á..; Bényei, G.; Jalsovszky, I.; Hackl, R.; Pekker, S.; Kamarás, K. Vibrational spectra of $C_{60}{\cdot}C_8H_8$ and $C_{70}{\cdot}C_8H_8$

in the rotor-stator and polymer phases. *J. Phys. Chem. B* **2007**, *111*, 12375–12382.

(29) Stepanian, S. G.; Karachevtsev, V. A.; Plokhotnichenko, A. M.; Adamowicz, L.; Rao, A. M. IR spectra of photopolymerized C_{60} films. Experimental and density functional theory study. *J. Phys. Chem. B* **2006**, *110*, 15769–15775.

Graphical TOC Entry